Melting of Magnesium Oxide to 2 TPa Using Double-Shock Compression

L. E. Hansen,[1,2] D. E. Fratanduono,[3] S. Zhang,[1] D. G. Hicks,[4] T. Suer,[1,5] Z. K. Sprowal,[1,2] M. F. Huff,[1,2] X. Gong,[1,6] B. J. Henderson,[1,2] D. N. Polsin,[1,6] M. Zaghoo,[1] S. X. Hu,[1,6] G. W. Collins,[1,2,6] and J. R. Rygg[1,2,6]

[1]Laboratory for Laser Energetics, University of Rochester
[2]Department of Physics and Astronomy, University of Rochester
[3]Lawrence Livermore National Laboratory
[4]Optical Sciences Centre, Swinburne University of Technology, Australia
[5]Department of Earth and Planetary Sciences, Harvard University
[6]Department of Mechanical Engineering, University of Rochester

Magnesium oxide (MgO, periclase) is an end-member of the (Mg, Fe)O magnesiowustite mineral, a major constituent of the Earth's lower mantle.[1,2] It is likely present in the deep interiors of gas giants such as Jupiter and Saturn and in rocky extra-solar planets known as super-Earths.[3,4] As an abundant component in planets, the physical properties of MgO can influence planetary structure and evolution. The B2 phase (CsCl type) of MgO is expected to be abundant in the mantles of super-Earths and in the rocky cores of gas giants due to the dissociation of $MgSiO_3$-perovskite.[4] The melting of MgO could therefore be an important driver of thermal and chemical exchange in the mantles and the core–mantle boundary regions of these planets.[5,6] Quantifying the melting behavior of MgO to the high pressures and temperatures of planetary interiors is therefore relevant to investigating a number of topical issues in planetary science.

The melt curve of MgO has been studied up to 40 GPa using laser- and resistance-heated diamond-anvil cells,[7–10] and up to 550 GPa on the principal Hugoniot with decaying-shock experiments.[11,12] Single shock waves can be used to study melting of a material to the pressure at which the principal Hugoniot crosses the melt curve; however, different experimental techniques are necessary to probe melting at higher pressures. In this work, we apply the double-shock self-impedance-matching technique[13,14] to measure the melt curve of MgO to 2 TPa—the highest pressure to which any material's melt curve has been studied experimentally.

These experiments were performed on the OMEGA EP Laser System.[15] The targets consisted of a 20-μm-thick CH polystyrene ablator, a 50-μm-thick quartz pusher, and a 100- or 200-μm-thick single-crystal $\langle 100 \rangle$ MgO sample. All pieces were laterally 3-mm squares. The target components were held together with 1 to 3 μm of low-viscosity epoxy. The quartz pusher produced steady shocks in the MgO sample and served as a temperature/reflectivity reference.[16,17] Two successive shock waves were launched into the sample with a dual laser pulse through ablation of the CH. The first shock was produced with 400 J in a single laser beam with a 6- or 4-ns flattop pulse (0.067 TW or 0.1 TW); the second shock was produced with a net 1500 to 6400 J in one to three beams with a 2-ns flattop pulse (0.75 to 3.2 TW). Distributed phase plates were used to create a spatially uniform irradiance profile with a 95% encircled energy spot diameter of 1100 μm. The time-resolved diagnostics included a streaked optical pyrometer (SOP)[18] and a dual-channel line-imaging VISAR (velocity interferometer system for any reflector).[19]

The measured first (black open circles) and second (red open and solid circles) shock pressure and temperature results are plotted in Fig. 1. At a phase boundary, a material's Hugoniot is often marked by a plateau or reversal in temperature with increasing pressure as thermal energy contributes to a phase transition.[20,21] This behavior has been observed in shock experiments on diamond,[22] SiO_2 (Ref. 17), and the principal Hugoniot of MgO.[11,12] Results of the second shock show a temperature increase of only 3000 K from 1.2 to 2 TPa; above this pressure, temperature rises rapidly. The three central second-shock data points (solid

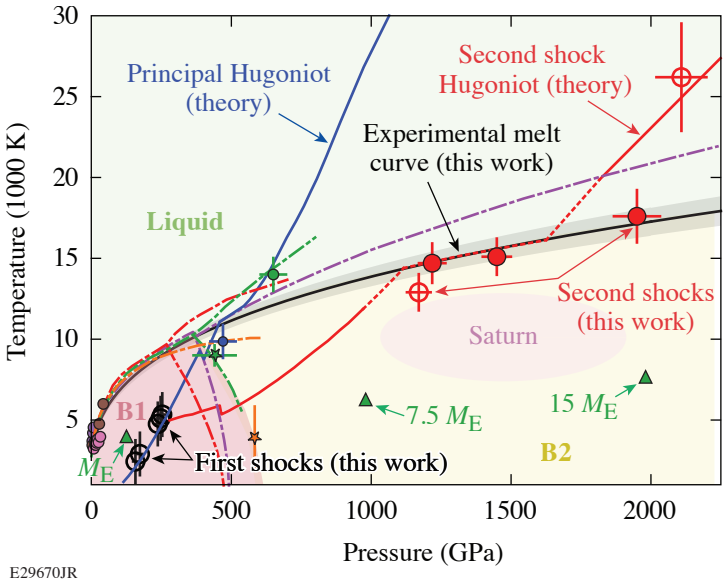

Figure 1
The phase diagram of MgO. Black open circles represent the first-shock B1 states in the present work. Red open and solid circles are the second-shock states; both pressure and temperature are measured. The three central second-shock states (solid red circles) are interpreted to be on the melting curve of MgO due to a lack of heating across a large increase in pressure. Melting data from previous experiments are plotted with small solid circles (pink,[7] purple,[9] brown,[10] green,[11] and blue[12]) and B1–B2 transition data are plotted with ×'s (green,[11] and orange[23]). Dotted–dashed curves are previously predicted phase boundaries (green,[13] red,[24] orange,[25] and purple[26]). The solid blue curve is a prediction for the principal Hugoniot,[26–28] and the solid red curve (interpolated with dashed red) is a prediction for the second shock Hugoniot.[26–29] The core–mantle boundary conditions are plotted for Saturn[30] and 1-, 7.5-, and 15-Earth-mass (M_E) super-Earths.[31] The solid black curve is the Simon–Glatzel fit [Eq. (1)] to the melting data in this work and lower-pressure anvil cell melt data,[8,10] with gray shading representing the uncertainty in the fit parameters.

red circles) are interpreted to lie on the melt curve of MgO because they demonstrate a lack of heating across a large increase in shock pressure, which is attributed to the latent heat of MgO melting. These experiments did not determine the structure of solid MgO, and no structural data exist at these pressures. It is assumed that the MgO melts from B2 in these experiments because no other solid phases are predicted above the B1–B2 transition.

To capture the shape of the high-pressure melt curve, we performed a fit to our data by combining select lower-pressure anvil cell melting data[8,10] with a Simon–Glatzel equation of the form

$$T_m[K] = 3098\left[\frac{P_m(\text{GPa})}{a} + 1\right]^{1/b}, \tag{1}$$

where T_m and P_m are the temperature and pressure of the melt curve and 3098 K is the melting temperature of MgO at atmospheric pressure.[8] This empirical relation has been used to describe the melting behavior of other oxides including SiO_2 (Ref. 15) and $MgSiO_3$ (Ref. 32). The best-fit parameters are given by a = 9.15 (2.23) GPa and b = 3.14 (0.19) with a covariance of –0.39, determined from a nonlinear least squares analysis. A previously published melting curve of MgO (Ref. 15) based on extrapolation of anvil-cell and decaying-shock melting data[8,9,11] overestimates the melting temperature at 1950 GPa by 27%. This simple fit was chosen based on the discrepancy in the melting temperature of MgO on the principal Hugoniot.

The melt curve in Eq. (1) is plotted in Fig. 1 (solid black) and shows strong agreement with recent density functional theory[26] (dashed–dotted purple curve) up to 650 GPa before the curves diverge. Reference 20 overestimates the measured melting temperature at 1950 GPa by 17%. The highest-pressure second-shock equation-of-state point in this work is in the liquid regime of the 173-GPa secondary Hugoniot of MgO and shows general agreement with first-principles equation-of-state simulations of secondary Hugoniots from similar initial shock conditions;[27–29] the slope of the secondary Hugoniot defined by the two highest-pressure second-shock points in this work does appear steeper than theoretical predictions. The discrepancy between experiment and theory on the melt curve could originate from the complex elastic and plastic responses of MgO during the shock/re-shock and phase transformation processes, which have not been considered in the first-principles calculations. This calls for larger-scale nonequilibrium simulations and crystallographic diagnostics to better understand problems as such. The low-pressure second-shock data in this work demonstrate that the double-shock technique is a valuable method for probing the behavior of MgO in the solid phase at the temperatures and pressures directly relevant to the core–mantle boundary of gas giants similar in size and composition to Saturn[30] and super-Earths in the 7.5- to 15-Earth-mass range.[31]

In summary, laser-driven double-shock compression is a valuable method for probing the behavior of MgO in the solid phase at extreme conditions. The present work uses this technique to extend the melting curve of MgO up to 2 TPa and 20,000 K, the highest pressures and temperatures to which any material's melt curve has been probed experimentally. These measurements allowed us to explore the state of the deep interiors of Saturn-sized gas giants and super-Earths. This technique can be used to further quantify the melting behavior of other planetary materials to further investigate the diversity of planetary structures. Additionally, the technique presented in this work will lead to new advances in probing phase transitions of transparent materials up to TPa pressures and significantly advance warm dense matter physics.

This material is based upon work supported by the Department of Energy National Nuclear Security Administration under Award Number DE-NA0003856, the University of Rochester, and the New York State Energy Research and Development Authority.

1. W. F. McDonough and S.-s. Sun, Chem. Geol. **120**, 223 (1995).
2. J.-Fu. Lin *et al*., Proc. Natl. Acad. Sci. **100**, 4405 (2003).
3. S. Seager *et al*., Astrophys. J. **669**, 1279 (2007).
4. K. Umemoto, R. M. Wentzcovitch, and P. B. Allen, Science **311**, 983 (2006).
5. L. Stixrude, Phil. Trans. R. Soc. A **372**, 20130076 (2014).
6. W. B. Tonks and H. J. Melosh, J. Geophys. Res. **98**, 5319 (1993).
7. A. Zerr and R. Boehler, Nature **371**, 506 (1994).
8. L. S. Dubrovinsky and S. K. Saxena, Phys. Chem. Minerals **24**, 547 (1997).
9. L. Zhang and Y. Fei, Geophys. Res. Lett. **35**, L13302 (2008).
10. Z. Du and K. K. M. Lee, Geophys. Res. Lett. **41**, 8061 (2014).
11. R. S. McWilliams *et al.*, Science **338**, 1330 (2012).
12. R. M. Bolis *et al.*, Geophys. Res. Lett. **43**, 9475 (2016).
13. M. Guarguaglini *et al.*, Phys. Plasmas **26**, 042704 (2019).
14. M. Guarguaglini *et al.*, Nat. Commun. **12**, 840 (2021).
15. D. D. Meyerhofer *et al*., J. Phys.: Conf. Ser. **244**, 032010 (2010).
16. S. Brygoo *et al*., J. Appl. Phys. **118**, 195901 (2015).
17. D. G. Hicks *et al*., Phys. Rev. Lett. **97**, 025502 (2006).
18. J. E. Miller *et al*., Rev. Sci. Instrum. **78**, 034903 (2007).
19. P. M. Celliers *et al*., Rev. Sci. Instrum. **75**, 4916 (2004).
20. S. B. Kormer, Sov. Phys.-Usp. **11**, 229 (1968).
21. G. A. Lyzenga, T. J. Ahrens, and A. C. Mitchell, J. Geophys. Res. **88**, 2431 (1983).
22. J. H. Eggert *et al*., Nat. Phys. **6**, 40 (2010).
23. F. Coppari *et al*., Nat. Geosci. **6**, 926 (2013).
24. S. Root *et al*., Phys. Rev. Lett. **115**, 198501 (2015).
25. N. de Koker and L. Stixrude, Geophys. J. Int. **178**, 162 (2009); **183**, 478(E) (2010).
26. F. Soubiran and B. Militzer, Phys. Rev. Lett. **125**, 175701 (2020).
27. F. Soubiran *et al*., J. Chem. Phys. **151**, 214104 (2019).
28. The principal and the second-shock Hugoniots at 20,000 K or higher are calculated by using the first-principles equation-of-state (FPEOS) database published in Refs. 27 and 29 for MgO. The initial conditions for the second shocks are estimated following the approach of S. Zhang, R. Paul, M. A. Morales, F. Malone, and S. X. Hu, in preparation. See the supplemental material for details.
29. B. Militzer *et al*., Phys. Rev. E **103**, 013203 (2021).
30. F. González-Cataldo, H. F. Wilson, and B. Militzer, Astrophys. J. **787**, 79 (2014).
31. F. W. Wagner *et al*., Astron. Astrophys. **541**, A103 (2012).
32. D. E. Fratanduono *et al*., Phys. Rev. B **97**, 214105 (2018).